Nucleus 4:4, 326–340; July/August 2013; © 2013 Landes Bioscience

# Trafficking of mRNAs containing ALREX-promoting elements through nuclear speckles

Abdalla Akef,[1] Hui Zhang,[1] Seiji Masuda[2] and Alexander F Palazzo[1,*]

[1]Department of Biochemistry; University of Toronto; Toronto, ON Canada; [2]Division of Integrated Life Science; Graduate School of Biostudies; Kyoto University; Kyoto, Japan

**Keywords:** nuclear speckles, mRNA nuclear export, poly(A)-tail, ALREX, TREX, UAP56, TAP/NXF1

**Abbreviations:** ALREX, alternative mRNA export; β*G*, beta-*Globin*; CTE, constitutive transport element; FISH, fluorescence in situ hybridization; *ftz*, *fushi tarazu*; HHT, homoharringtonine; *INS*, *insulin*; *MHC*, *major histocompatibility complex*; mRNP, messenger ribonucleoprotein; MSCR, mitochondrial-targeting sequence coding region; ORF, open reading frame; PolII, RNA polymerase II; RT-qPCR, reverse transcription–quantitative polymerase chain reaction; TREX, transcription export; shRNA, small hairpin RNA; SRP, signal recognition particle; SSCR, signal sequence coding region

In vertebrates, the majority of mRNAs that encode secreted, membrane-bound or mitochondrial proteins contain RNA elements that activate an alternative mRNA nuclear export (ALREX) pathway. Here we demonstrate that mRNAs containing ALREX-promoting elements are trafficked through nuclear speckles. Although ALREX-promoting elements enhance nuclear speckle localization, additional features within the mRNA largely drive this process. Depletion of two TREX-associated RNA helicases, UAP56 and its paralog URH49, or inhibition of the TREX-associated nuclear transport factor, TAP, not only inhibits ALREX, but also appears to trap these mRNAs in nuclear speckles. mRNAs that contain ALREX-promoting elements associate with UAP56 in vivo. Finally, we demonstrate that mRNAs lacking a poly(A)-tail are not efficiently exported by the ALREX pathway and show enhanced association with nuclear speckles. Our data suggest that within the speckle, ALREX-promoting elements, in conjunction with the poly(A)-tail, likely stimulate UAP56/URH49 and TAP dependent steps that lead to the eventual egress of the export-competent mRNP from these structures.

## Introduction

In eukaryotes, mRNAs are synthesized in the nucleus where they are capped, spliced, and polyadenylated. During these maturation steps, the mRNAs are loaded with several proteins to form messenger Ribonucleoprotein (mRNP) particles that are capable of crossing the nuclear pore to reach the cytoplasm where the mRNAs are translated into proteins.[1] It is believed that the majority of mRNAs in vertebrate cells are exported from the nucleus in a splicing dependent export pathway.[2] This pathway is initiated during splicing of the first intron where the spliceosome and the nuclear cap binding complex collaborate to deposit the transcription export (TREX) complex at the 5'end of the mRNA.[3,4] TREX is a multiprotein complex that is composed of the THO subcomplex, the RNA helicase UAP56, the adaptor molecules Aly and Chtop.[5-8] This complex acts to recruit the heterodimeric mRNA export receptor TAP/p15 (TAP is also known as NXF1), which directly binds to the mRNA[9] and ferries it across the nuclear pore to the cytoplasm.[10-12]

In addition to the canonical splicing-dependent pathway, several unconventional mRNA export mechanisms have been characterized. Previously, we reported that the presence of a signal sequence coding region (SSCR) or a mitochondrial-targeting sequence coding region (MSCR) at the beginning of the open reading frame (ORF) of an mRNA promotes the Alternative mRNA Export (ALREX) pathway in vertebrate cells.[13,14] In addition to coding for targeting peptides to the endoplasmic reticulum and the mitochondrion respectively, the SSCR and MSCR act as RNA elements that facilitate the nuclear export of their transcripts independently of splicing or a functional 5' cap.[13] These export-promoting SSCRs and MSCRs tend to be depleted of adenines and present within the first exon. ALREX-promoting SSCRs also enhance translation of the mRNA, and this likely requires a rearrangement of mRNP components at the cytoplasmic face of the nuclear pore after the completion of nuclear export.[15]

Presumably ALREX-elements function in export by regulating the composition of the mRNP within the nucleus. ALREX requires TAP/p15[13,14] and ALREX-elements likely recruit this nuclear transport receptor to the mRNP through an adaptor molecule. However, little else is known about how these sequences influence mRNP formation. In addition, it is unclear where in the nucleoplasm the assembly of these mRNPs takes place. One potential subnuclear compartment where mRNP assemly may occur is nuclear speckles. These are large nuclear aggregates that contain active RNA polymerase II (PolII), spliceosomal

*Correspondence to: Alexander F. Palazzo; Email: alex.palazzo@utoronto.ca
Submitted: 05/08/13; Revised: 07/31/13; Accepted: 08/05/13
http://dx.doi.org/10.4161/nucl.26052

components, and splicing cofactors such as SR proteins.[16] In addition, these structures contain TREX complex components.[3,5,17,18] Many mRNAs appear to be recruited to nuclear speckles by the act of splicing.[19-22] In the vicinity of speckles, splicing is completed and the mRNA acquires components of the exon junction and likely TREX complexes.[23-25] Depletion of UAP56, enhances the association of these spliced mRNAs with nuclear speckles,[22] suggesting that TREX is required for mRNAs to exit these structures. Finally, it is likely that TAP/p15 is itself loaded onto spliced transcripts within or in the vicinity of nuclear speckles.[24,26] In contrast, intronless transcripts, including those that originate from naturally intronless genes, do not appear to associate with nuclear speckles.[22,27,28] Since many of these mRNAs are well exported, it is likely that mRNA-trafficking through these structures is not absolutely required for assembling an export-competent mRNP.

Here we characterize some of the earliest events in mRNP assembly as promoted by the ALREX pathway. Our data indicates that mRNAs containing ALREX-promoting elements are initially targeted to nuclear speckles, and this may be promoted by multiple attributes, which include splicing, ALREX-promoting elements, and other undetermined features that are present in certain transcripts. Our data suggests that within speckles, mRNAs containing ALREX-promoting elements undergo a series of mRNP maturation steps. One nuclear speckle step likely involves the recruitment of the RNA helicases UAP56 and URH49 to the mRNA. A second downstream step requires TAP activity. In addition, our data suggests that the poly(A)-tail is also required for a nuclear speckle-associated event. In summary, our data supports the model that the initial targeting of mRNA to nuclear speckles licenses an mRNA to use the ALREX pathway.

## Results

**Nuclear speckle association is promoted by sequences within the reporter transcript and by the *MHC* SSCR.** To understand the early steps of the ALREX pathway, we monitored the distribution of newly synthesized mRNA that contains or lacks an ALREX-promoting SSCR. We first investigated different versions of the intronless *fushi tarazu* (*ftz*) reporter mRNA which either possesses (*MHC-ftz-*Δ*i*) or lacks (*c-ftz-*Δ*i*) the SSCR from the mouse *Major Histocompatibility Complex* (*MHC*) *H2kb* gene. This SSCR promotes efficient nuclear export by the ALREX pathway.[13]

We thus microinjected plasmids that contained either version of *ftz* into the nucleus of human osteosarcoma cells (U2OS) and after various periods of time we imaged the endogenously synthesized mRNA by fluorescence in situ hybridization (FISH) and various subcellular markers by immunofluorescence. Both *MHC-ftz-*Δ*i* and *c-ftz-*Δ*i* mRNAs appeared to associate with foci within the nucleus that were reminiscent of nuclear speckles, also known as interchromatin granules.[16] This observation, was at odds with previously published findings that indicated that the ability for mRNAs to associate with these structures required an intron and was dependent on splicing.[19-22] In several of these studies, an intron-containing, but not an intronless version, of the human β-*Globin* (β*G*) transcript was targeted to speckles. We thus compared the distribution of mRNA transcribed from microinjected plasmids containing either *MHC-ftz-*Δ*i*, *c-ftz-*Δ*i*, or β*G-*Δ*i* (an intronless version of the β*G* gene), and examined their association with nuclear speckles over time. We observed that both *MHC-ftz-*Δ*i* and *c-ftz-*Δ*i* colocalized with SC35, a marker of nuclear speckles,[29,30] however this association was only apparent after at least 30 min of expression (**Fig. 1A**, compare the distribution of *MHC-ftz-*Δ*i* with SC35 at 15 min and 1 h post-microinjection, arrows indicate examples of nuclear speckles enriched with *MHC-ftz-*Δ*i* or *c-ftz-*Δ*i* mRNAs). This colocalization was confirmed by line scans (**Fig. 1B**). In contrast, β*G-*Δ*i*, mRNA displayed little to no colocalization with SC35 (**Fig. 1A and B**), as previously reported.[21,22]

In order to quantify the enrichment of the various mRNAs with nuclear speckles, we assessed the Pearson correlation coefficient (R) between the mRNA FISH stain and SC35 immunofluorescence in individual speckles. This analysis indicates the degree of mRNA enrichment in each nuclear speckle as compared with the surrounding regions. Examples of highly correlated ($R > 0.8$), weakly correlated ($0.8 > R > 0.5$) and non-correlated ($R < 0.5$) distributions are shown in **Figure 1C**. This analysis confirmed that all of the different *ftz* transcripts, but not β*G-*Δ*i,* strongly associated with nuclear speckles. To obtain a control for random colocalization, we also examined the correlation between microinjected fluorescent 70 kDa dextran and SC35, and these did not significantly overlap (**Fig. 1D**; **Fig. S1**). As a further control, we estimated the degree of random colocalization by overlaying each FISH nuclear image onto an SC35 immunofluorescence image, which was obtained from a different nucleus and then repeated the Pearson correlations analysis. Again we did not detect any significant colocalization (**Fig. 1E**). Interestingly, our analysis indicated that β*G-*Δ*i* displayed weak association with speckles that was above background [i.e., colocalization between dextran and SC35 (**Fig. 1D**), and colocalization between β*G* FISH and SC35 from different nuclei (**Fig. 1E**)].

To determine the effect of ALREX-promoting SSCRs on this process we inserted the mouse *MHC* SSCR into the 5'end of the intronless β*G* gene (creating *MHC*-β*G-*Δ*i*, see **Fig. 2A**) and monitored its ability to localize to speckles. As a control we also examined a version of β*G* that contains its two natural introns (β*G-i*). The insertion of *MHC* SSCR had only a moderate effect on speckle localization (**Fig. 1F**, compare *MHC*-β*G-*Δ*i* to β*G-*Δ*i*). As previously reported,[19,21,22] the insertion of an intron had a more pronounced effect (**Fig. 1F**, compare β*G-i* to β*G-*Δ*i*). These results suggested that the *MHC* SSCR promotes weak speckle association. To determine whether other ALREX-sensitive mRNAs associate with speckles, we next examined an intronless version of the human *insulin* (*INS-*Δ*i*) transcript. This mRNA is efficiently exported and this activity is sensitive to mutations within its SSCR.[13] Indeed, this intronless mRNA was enriched in speckles to a higher degree than all the other transcripts (**Fig. 1F**). Furthermore, disruption of the *insulin* SSCR with 5 silent adenine substitutions (*5A-INS-*Δ*i*) slightly decreased, but did not abolish, speckle localization (**Fig. 1F**), despite the fact these mutations partially inhibit nuclear export.[13]

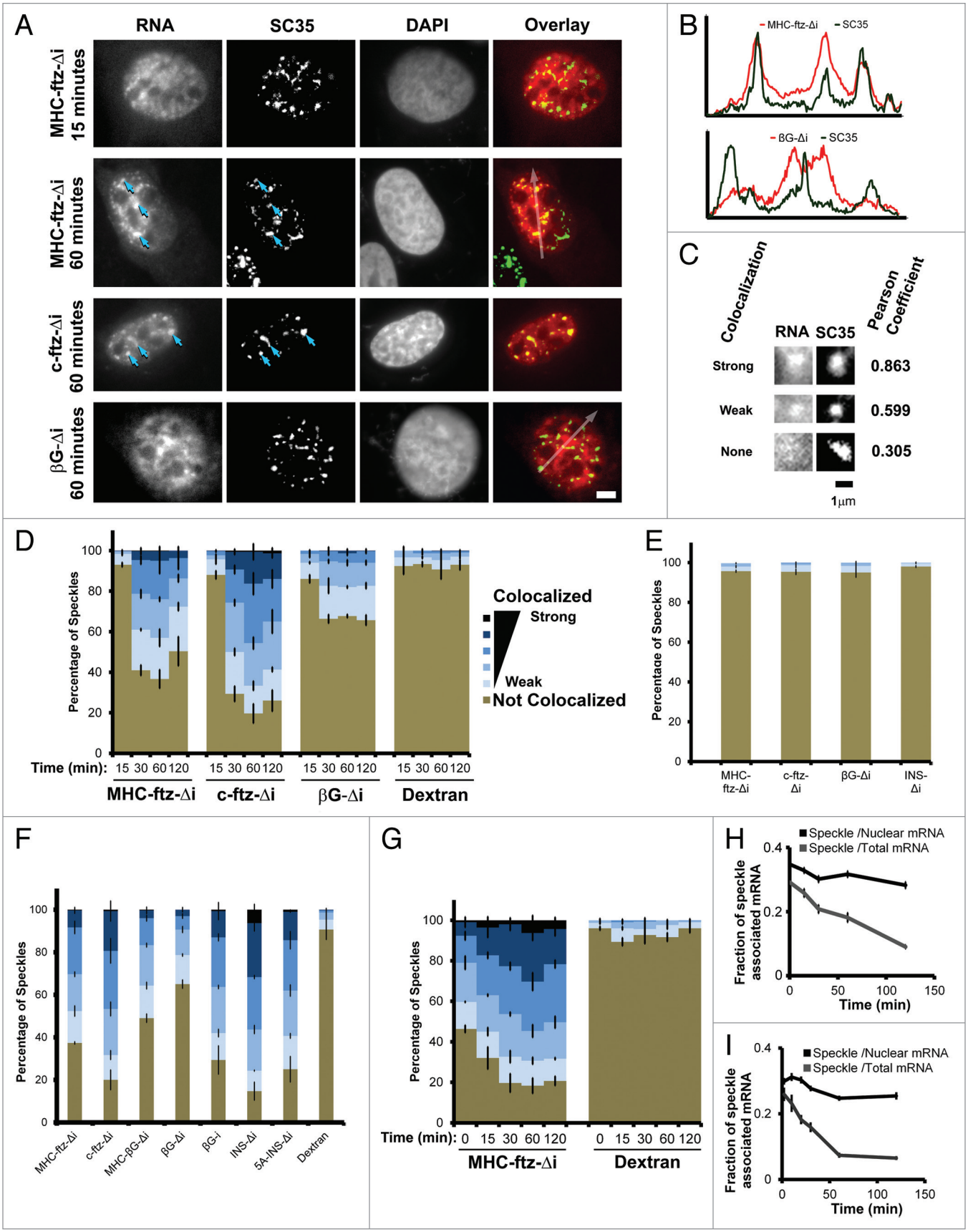


**Figure 1.** For figure legend, see page 329.

**Figure 1 (See opposite page).** Analysis of mRNA localization to nuclear speckles. (**A**) U2OS cells were microinjected with plasmids containing the *MHC-ftz-Δi*, *c-ftz-Δi* or *βG-Δi* constructs. After allowing expression for the indicated time points, the cells were fixed, probed for *ftz* or *βG* mRNA by FISH, immunostained for the nuclear speckle marker SC35 and stained for DNA using DAPI. Each row represents a single field of view. An overlay of the mRNA (red) and SC35 (green) is shown in the right panels. Scale bar = 5 μm. (**B**) The fluorescence intensities (*y*-axis) of mRNA (*MHC-ftz-Δi* top panel and *βG-Δi,* lower panel; red) and SC35 (green) were plotted along the length of the arrows (x-axis) as seen in the overlay images in (**A**). (**C**) Representative examples of strong, weak and non-colocalization of mRNA and SC35. Again each row represents a single field of view. The Pearson correlation coefficient for each pair of images is shown on the right. Scale bar of 1 μm is shown. (**D**) U2OS cells were microinjected with various plasmids. After allowing expression for the indicated time points, the cells were fixed, probed and imaged as in (**A**). For each time point, the percentage of SC35-positive nuclear speckles that colocalized with *MHC-ftz-Δi*, *c-ftz-Δi* and *βG-Δi* mRNAs, was plotted. As a control, the percentage of speckles showing different levels of colocalization with the microinjection marker, 70 kDa Dextran conjugated to Oregon Green was also analyzed. Speckles were binned into 6 categories based on their Pearson correlation coefficient ("Strong colocalization," R > 0.9; R = 0.9–0.8; R = 0.8–0.7; R = 0.7–0.6; "Weak colocalization," R = 0.6–0.5; "Not colocalized" R < 0.5). Each column represents the average of three experiments, each consisting of 100 SC35-positive speckles (see methods section for more details). Error bars represent standard error of the mean. (**E**) For each mRNA, FISH images from one set of nuclei (1 h post-microinjection), were superimposed over SC35 images from a separate set of un-injected nuclei to determine the rate of random colocalization. The data was analyzed and plotted as in (**D**). (**F**) The percentage of speckles that colocalized with different transcripts was plotted for cells, 1 h after microinjection of plasmids. Again, the data was analyzed and plotted as in (**D**). (**G and H**) Plasmids containing the *MHC-ftz-Δi* gene were microinjected into the nuclei of U2OS cells and mRNA was allowed to express for 20 min. Cells were then treated with α-amanitin and the colocalization of *MHC-ftz-Δi* mRNA with SC35 over time (post-drug treatment, indicated on the *x*-axes) was monitored. (**G**) The percentage of nuclear speckles that demonstrate different levels of colocalization with *MHC-ftz-Δi.* Again, the data was analyzed and plotted as in (**D**). (**H**) The amount of *MHC-ftz-Δi* mRNA that is present in nuclear speckles (as defined by the brightest 20% pixels in the nucleus, using SC35 immunofluorescence) as a percentage of either the cellular or nuclear level. Each data point represents the average and standard error of the mean of 10 cells. (**I**) In vitro transcribed *MHC-ftz-Δi* mRNA was microinjected into the nuclei of U2OS cells. Cells were left for various amounts of time to allow mRNA export. The amount of *MHC-ftz-Δi* mRNA present in nuclear speckles was monitored as described in **Figure 1H**.

From these observations we conclude that various reporter mRNAs appear to have different abilities to localize to nuclear speckles. We can also conclude that the ability to associate with nuclear speckles is not sufficient for mRNAs to be efficiently exported from the nucleus, as exemplified by *c-ftz-Δi*. Furthermore, our data indicates that although ALREX-elements may have some intrinsic ability to promote the localization of mRNAs to nuclear speckles, robust speckle targeting requires the presence of supplementary features within the transcript.

***MHC-ftz-Δi* traffics through nuclear speckles.** We next investigated whether these mRNAs could target to the speckles post-transcriptionally. To test this idea we microinjected plasmids containing *MHC-ftz-Δi* and after 20 min we added α-amanitin to the cells. This treatment completely inhibits transcription of microinjected plasmids within 5 min.[31] We then monitored the distribution of *MHC-ftz-Δi* at various time points after transcriptional shut-down. Our analysis indicated that over time, newly synthesized *MHC-ftz-Δi* transcripts increased their degree of colocalization with SC35 (**Fig. 1G**), suggesting that they can target to these structures post-transcriptionally.

Although colocalization studies indicate whether a particular mRNA is enriched in speckles, this does not indicate how much of that particular transcript partitions into these structures. Moreover, monitoring the total level of speckle-associated mRNA over time may provide insights into the kinetics of this process. To examine whether the localization to speckles represented a transient event, we used the SC35 immunofluorescence signal to subdivide nuclei into nuclear speckle regions and non-speckle regions (for details see the methods section) and monitored what fraction of *MHC-ftz-Δi* was present in these zones after α-amanitin treatment. To limit the amount of variation between measurements, nuclear speckles were defined by thresholding the brightest 20% (± 0.5%) of pixels in each nucleus using SC35 immunofluorescence. Generally, the total amount of speckle-associated *MHC-ftz-Δi* mRNA decreased over time (**Fig. 1H**, see Speckle /Total mRNA). This result implied that this mRNA was trafficking out of the nuclear speckles over the time course. Interestingly, when only the nuclear *MHC-ftz-Δi* mRNA levels were assessed, the amount associated with speckles only slightly decreased over the same period (**Fig. 1H**, Speckle/Nuclear mRNA). From these measurements, we could not definitively determine whether any of the mRNA in the speckle was targeted post-transcriptionally. However this data suggested that the partitioning of mRNA between the non-speckle and speckle regions was close to equilibrium.

To obtain a clearer picture of post-transcriptional mRNA trafficking through nuclear speckles, we microinjected in vitro synthesized, capped, and polyadenylated mRNA into nuclei and measured the partitioning of this into speckles over time. Note that microinjected mRNA is exported at a higher rate than endogenously transcribed transcripts. For example, the half-time of export for microinjected *MHC-ftz-Δi* mRNA is about 15 min, while the figure for the same mRNA that is transcribed endogenously off of plasmids is 40–50 min.[13] This also holds true for splicing dependent export (Akef A and Palazzo A, unpublished observations). We found that microinjected *MHC-ftz-Δi* mRNA very rapidly accumulated into nuclear speckles, and this peaked at about 10 min post injection (**Fig. 1I**, Speckle /Nuclear mRNA). After this point the amount of mRNA in nuclear speckles decreased. This result confirmed that mRNA was likely trafficking through nuclear speckles and that this localization could occur post-transcriptionally.

In summary our data suggests that many intronless mRNAs traffic through nuclear speckles. In light of the role of nuclear speckles in mRNA metabolism,[16] it is likely that this trafficking is linked to mRNP assembly. Nonetheless, we cannot exclude the possibility that only a fraction of the *MHC-ftz-Δi* mRNA transits through speckles.

**The extent of nuclear export promoted by the *MHC* SSCR varies between reporter mRNAs.** Since *MHC-βG-Δi* mRNA

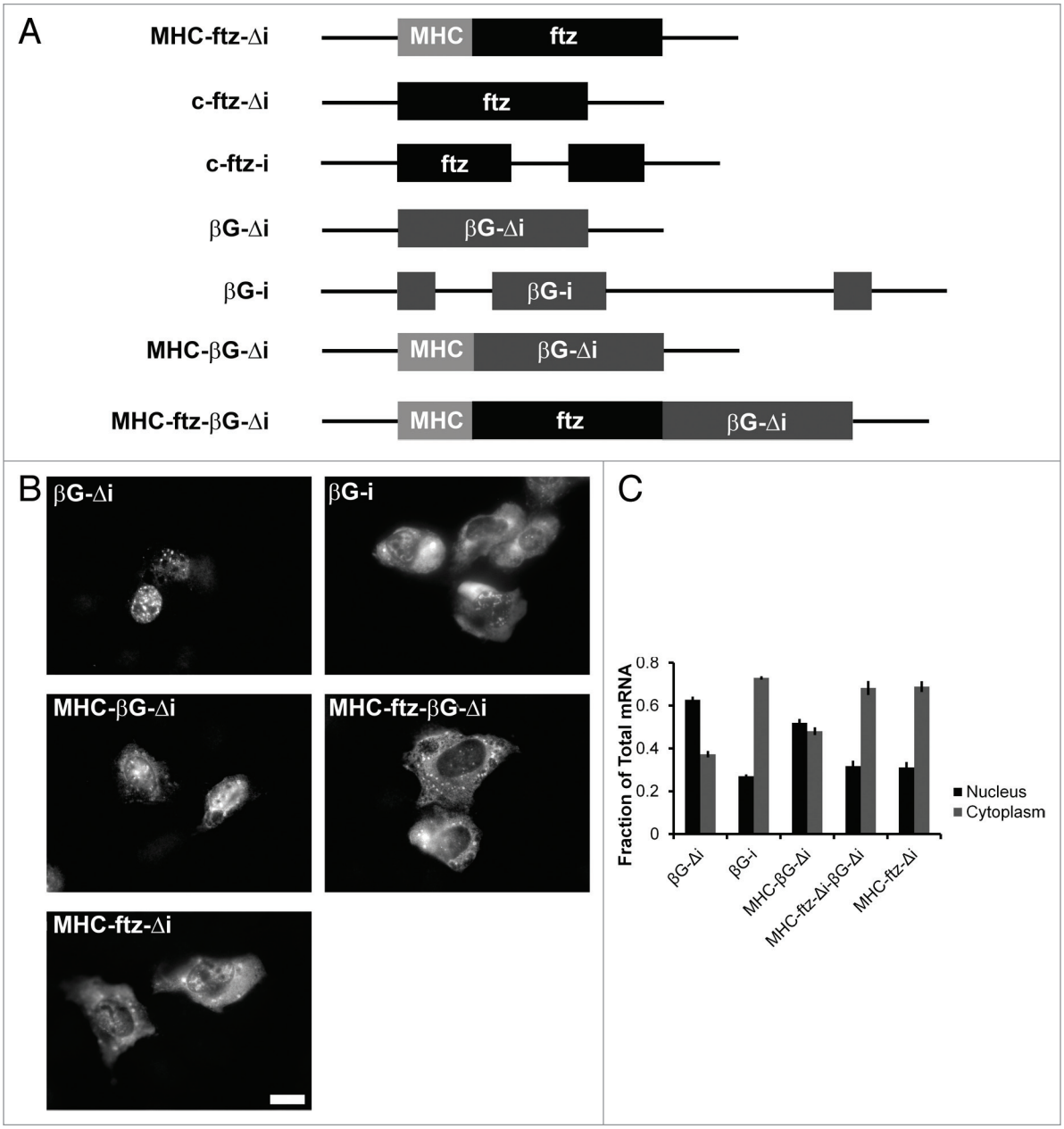


**Figure 2.** The extent of nuclear export promoted by the *MHC* SSCR varies between reporter mRNAs. (**A**) Schematic representation of the different constructs used in this study. (**B and C**) Plasmids containing the indicated constructs were microinjected into the nuclei of human U2OS cells. After 20 min, cells were treated with α-amanitin and mRNA export was allowed to proceed for 2 h. Cells were then fixed, probed for *ftz* or β*G* mRNA by FISH, imaged (**A**) and nuclear export was quantified (**B**). Scale bar = 20 μm. Each bar represents the average and standard error of three independent experiments, each consisting of 15–60 cells.

had relatively weak targeting to nuclear speckles, we wondered whether it was efficiently exported. To test this idea we monitored the nuclear export of various versions of β*G* mRNAs (see **Fig. 2A**) using a standard microinjection based assay.[31]

DNA plasmids that contained these various genes were injected into U2OS nuclei along with a 70 kDa fluorescently labeled dextran, which cannot passively cross the nuclear pore and thus be used as a marker for injected cells. After 20 min, the RNA PolII inhibitor α-amanitin was added to halt further transcription. Cells were left for 2 h to allow the newly synthesized mRNA to be exported. Subsequently, cells were fixed and processed for FISH. Interestingly, the *MHC* SSCR promoted export of β*G*, but this was substantially weaker than the export promoted splicing (compare *MHC*-β*G*-Δ*i*, β*G*-Δ*i*, and β*G*-*i*, **Fig. 2B and C**). In contrast, and as previously reported,[13] the *MHC* SSCR containing *ftz* transcript was efficiently exported to the cytoplasm (**Fig. 2B and C**). This result suggested that these two reporter constructs (i.e., *ftz* and β*G*) are not equivalent.

Interestingly, *c-ftz*-Δ*i* mRNA encodes an unstable protein (Palazzo A, unpublished observations), raising the possibility that

it is eliminated by some quality control mechanism. To ensure that *c-ftz-Δi* was not degraded co-translationally, we treated cells with the translation inhibitor homoharringtonine (HHT) for 30 min before injecting plasmids containing *MHC-ftz-Δi* or *c-ftz-Δi*. HHT-treatment had no effect on the level of nuclear export of either mRNA (**Fig. S2A and B**). In order to ensure that translation was inhibited, we took advantage of the fact that the *ftz* reporter encodes a protein fused to an HA epitope and immunostained *MHC-ftz-Δi* injected cells. As expected, treating cells with HHT greatly diminished the HA immunofluorescence (**Fig. S2C**).

The lack of efficient export by *MHC-βG-Δi* could be explained by two possible models: either *βG* contained anti-ALREX activity, or *ftz* contained one, or several, features that potentiate ALREX. To test these models, we fused the two genes (creating *MHC-ftz-βG-Δi*, see **Fig. 2A**) and measured the export of the resulting mRNA. We found that this transcript was efficiently exported (**Fig. 2B and C**), indicating that *ftz* contained some feature that was required for ALREX.

From these experiments we conclude that the *MHC* SSCR promotes nuclear export of various reporter mRNAs, but that the amount of activity may differ. This variation is unlikely to be related to the translational products of the different transcripts. Instead our results are consistent with the model that certain reporters contain additional features that license an mRNA for ALREX. These features may be related to the propensity of a given transcript to localize to nuclear speckles.

**The nuclear export of *MHC-ftz-Δi* requires UAP56 and URH49.** Recent studies have suggested that TREX components are required for spliced mRNAs to exit nuclear speckles.[22] Previously, we demonstrated that in HeLa cells the co-depletion of the RNA DExD/H-box helicase UAP56, and its close paralog URH49, only partially inhibited the export of microinjected *MHC-ftz-Δi* mRNA.[13] In contrast the export of *c-ftz-i* was more drastically affected.[13] These previous experiments were hampered by the fact that at the time we did not have access to an antibody specific for URH49 and thus could not determine the efficiency of its knockdown.

In light of our localization findings, we decided to revisit these experiments, but this time monitoring the export of endogenously transcribed mRNAs. We took advantage of a lentiviral delivery system to transduce U2OS with plasmids that contain small hairpin RNA (shRNA) constructs that are complementary in sequence to both UAP56 and URH49 mRNAs. As shown in **Figure 3A**, treating cells with these two viruses for three days caused a decrease in the level of UAP56 and URH49 protein levels in comparison to cells which were treated with control viruses (UAP56 levels decreased by 73 ± 7%, while URH49 decreased 87 ± 3%, n = 3). These cells were microinjected with plasmids containing *MHC-ftz-Δi* or *c-ftz-i*. After allowing transcription to proceed for 20 min, α-amanitin was added to shut off transcription, and the newly synthesized mRNA was allowed to export for an additional 2 h. We observed that when UAP56 and URH49 were co-depleted, both *MHC-ftz-Δi* and *c-ftz-i* mRNAs were fully retained in the nucleus (**Fig. 3B**, quantitation **Fig. 3C**). In contrast, depletion of either helicase alone had only slight effects on export, although *c-ftz-i* appeared to be more sensitive to UAP56 depletion than *MHC-ftz-Δi* (**Fig. 3C**). As previously published,[32] co-depletion of UAP56 and URH49 also caused a drastic accumulation of poly(A) mRNA in the nucleus (**Fig. 3F**). In contrast, depletion of either UAP56 or URH49 alone did not cause a change in poly(A) mRNA distribution. Depletion of the THO complex member THOC1 (also known as hHpr1 and p84) or the adaptor Aly had little to no effect on the export of either *MHC-ftz-Δi* or *c-ftz-i* mRNA (**Fig. 3C–E**). Furthermore, depletion of either THOC1 or Aly also had no effect on bulk mRNA export (**Fig. 3F**).

In light of these results we wanted to revisit our previous experimental results investigating the export of in vitro synthesized mRNAs in HeLa cells depleted of UAP56 and URH49.[13] One difference between our previous experiments and our current results is the use of α-amanitin in the latter. Nevertheless, when α-amanitin treatment was omitted from DNA injection experiments, *MHC-ftz-Δi* mRNA was still retained in the nucleus in U2OS cells depleted of UAP56 and URH49 (**Fig. 3G**). It is possible that microinjected mRNA, which is exported more rapidly than its in vivo transcribed counterpart, is more efficient at utilizing the low levels of UAP56/URH49 remaining in cells, regardless of the cell line. Indeed, the export of microinjected *MHC-ftz-Δi* mRNA was only partially inhibited in U2OS cells that were depleted of UAP56 and URH49 (**Fig. 3H**), confirming what we previously reported in HeLa cells. In contrast, the export of microinjected *c-ftz-i* mRNA was more sensitive to the depletion of these two factors.

From these experiments we conclude that both ALREX and the splicing dependent export pathways are mediated by UAP56 and URH49. Furthermore, our data suggests that ALREX may require lower levels of these two helicases than splicing dependent export.

**UAP56, URH49, and TAP/p15 are required for *MHC-ftz-Δi* to exit out of nuclear speckles.** In the course of our experiments we observed that the depletion of UAP56 and URH49 caused *MHC-ftz-Δi* mRNAs to accumulate into large nuclear foci and these colocalized with several nuclear speckle markers such as SC35 and Aly (**Fig. 4A and B**). In agreement with previous findings,[22] *c-ftz-i* also accumulated in nuclear speckles in UAP56/URH49-depleted cells (**Fig. 4C**). The speckle localization of *MHC-ftz-Δi* was much more pronounced in the UAP56/URH49 knockdown cells than in control cells, whether this was calculated by Pearson correlation or by computing the total amount of mRNA associated with these structures (**Fig. 4D and E**). Indeed, in the knockdown cells practically every SC35-positive speckle had an enrichment of *MHC-ftz-Δi* mRNA (**Fig. 4D**). In contrast, the depletion of these two helicases had only minor effects on the speckle-association of *βG-Δi* mRNA (**Fig. 4D and F**).

Since TAP/p15 is also thought to associate with mRNA in nuclear speckles,[24,26] and its activity is required for ALREX,[13,14] we next assessed whether inhibition of this protein also resulted in the accumulation of *MHC-ftz-Δi* mRNAs in these structures. When plasmids containing the *MHC-ftz-Δi* gene were co-injected with RNA that contained the constitutive transport element (CTE), a viral sequence that prevents TAP from

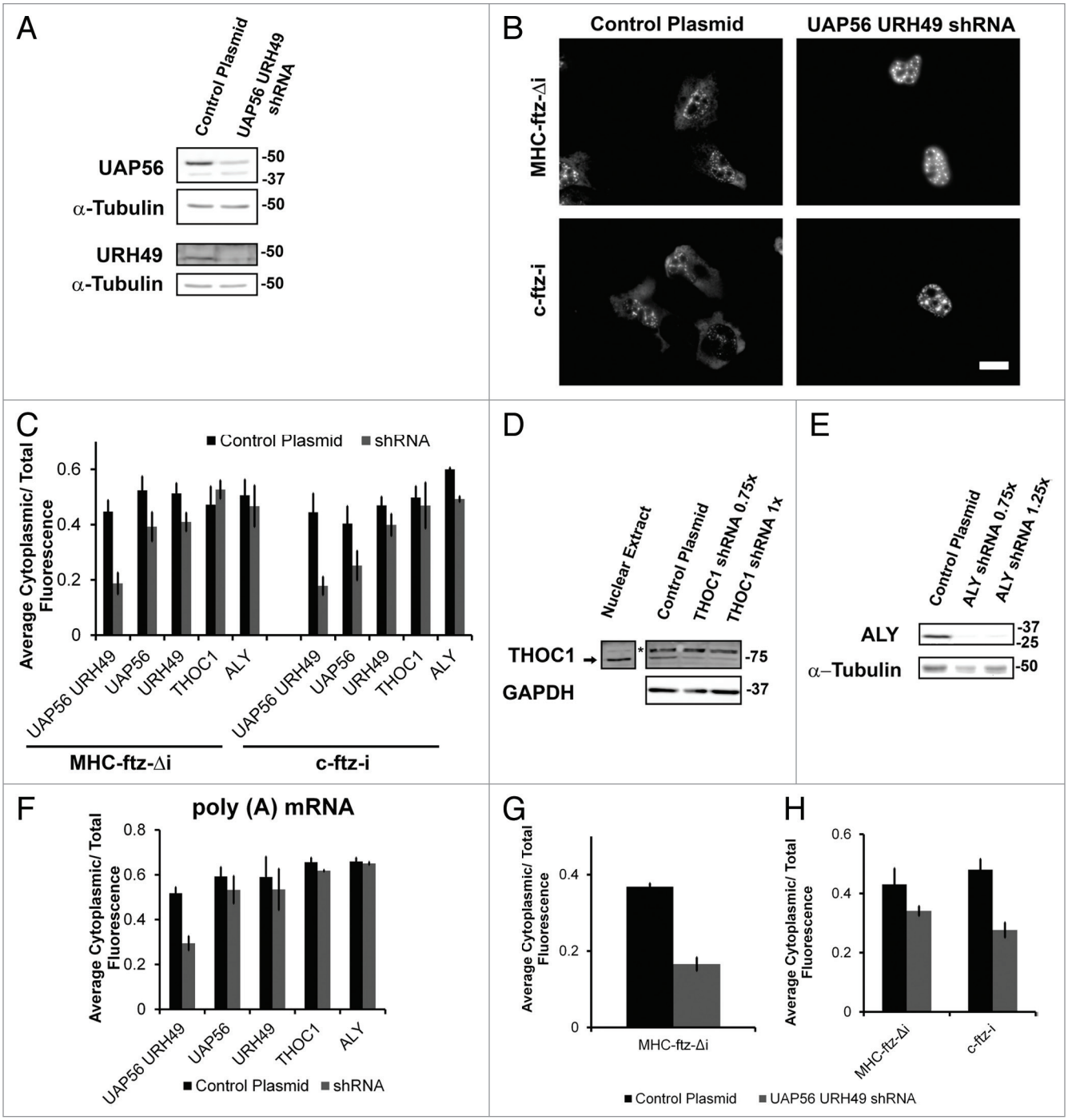


**Figure 3.** For figure legend, see page 333.

associating with mRNA substrates,[33] not only was the nuclear export of *MHC-ftz-Δi* inhibited, but this mRNA also accumulated into speckles to a much higher degree than in control cells (**Fig. 5A–C**). To confirm our results we also examined *INS-Δi*. Indeed, CTE co-injection also inhibited its export (**Fig. 5D**) and enhanced its association with speckles (**Fig. 5B and E**).

These experiments indicate that mRNAs containing ALREX-elements require both UAP56/URH49 and TAP/p15 for nuclear export. Although it is possible that inhibition of TREX-components directly promotes the targeting of mRNA to speckles, we favor the model that under normal conditions these proteins enhance the rate of egress from nuclear speckles.

**UAP56 associates with *MHC-ftz* mRNA.** In U2OS cells, UAP56 is distributed throughout the nucleoplasm with a slight enrichment in nuclear speckles (**Fig. S3A**). However, upon UAP56/URH49 co-depletion, the remaining UAP56 was predominantly associated with nuclear speckles (**Fig. S3A**). Interestingly this change in distribution was seen across almost

**Figure 3 (See opposite page).** UAP56 and URH49 are required for the export of *MHC-ftz-Δi*. (**A**) U2OS cells were treated with lentiviruses that mediate the delivery of either plasmids that contain shRNAs directed against UAP56 and URH49 or an empty control plasmid. Cell lysates were collected after 72 h, separated by SDS-PAGE and analyzed by immunoblotting using antibodies against UAP56, URH49 and α-tubulin. (**B and C**) U2OS cells depleted of various proteins 72 h (for UAP56 and URH49) or 96 h (for THOC1 or Aly) post-infection were microinjected with plasmids containing *MHC-ftz-Δi* or *c-ftz-i*. After allowing expression for 20 min, cells were treated with α-amanitin and allowed to export the mRNA for an additional 2 h. Cells were then fixed, and the mRNA was stained by FISH (**B**). Scale bar = 20 μm. (**C**) Quantification of the fraction of *MHC-ftz-Δi* and *c-ftz-i* mRNA in the cytoplasm. Each bar represents the average and standard error of at least three independent experiments, each consisting of 15–30 cells. Note that for each experiment, depleted and control cells were assayed in parallel to control for day-to-day variations in nuclear export levels. (**D and E**) U2OS cells were treated with lentiviruses that mediate the delivery of shRNAs directed against THOC1 (**D**), Aly (**E**) or an empty plasmid (**D and E**). Cell lysates were collected after 96 h, separated by SDS-PAGE and analyzed by immunoblotting with antibodies against THOC1, Aly, GAPDH and tubulin. Asterisk represents a non-specific band that is absent from HeLa nuclear extract. To account for unequal cell confluency several volumes of the knock-down lysate were loaded (0.75 ×, 1 ×, or 1.25 × of the control cell lysate). (**F**) Quantification of the fraction of poly(A) mRNA in the cytoplasm in cells co-depleted of UAP56 and URH49, or depleted of UAP56, URH49, THOC1 or Aly, or treated with control lentiviruses. Each bar represents the average and standard error of at least three independent experiments, each consisting of 15–30 cells. (**G**) U2OS cells co-depleted of UAP56 and URH49, or treated with control lentiviruses, were microinjected with DNA plasmids containing *MHC-ftz-Δi*. Cells were fixed two hours after injection without the prior addition of the transcription inhibitor α-amanitin and the mRNA was stained by FISH. Quantification of the fraction of cytoplasmic mRNA is shown. Each bar represents the average of at least three independent experiments, each consisting of 11–30 cells. Error bars represent standard error of the mean. (**H**) U2OS cells co-depleted of UAP56 and URH49, or treated with control lentiviruses, were microinjected with either in vitro transcribed and polyadenylated *MHC-ftz-Δi* or *c-ftz-i* mRNA. Cells were fixed 1 h after microinjection and the mRNA was stained by FISH. Quantification of the cytoplasmic mRNA distribution is shown. Each bar represents the average and standard deviation of two independent experiments, each consisting of 9–25 cells.

the entire cell population (**Fig. S3B**). Since this shRNA treatment also promoted the enrichment of *MHC-ftz-Δi* in speckles, we decided to determine whether UAP56 associates with this mRNA in vivo. Previously, it had been demonstrated that UAP56 is recruited to mRNAs in a splicing dependent manner using an in vitro splicing reaction.[3] We thus immunoprecipitated UAP56 from cells expressing various *ftz* constructs and analyzed the interacting RNAs by reverse transcription-quantitative PCR (RT-qPCR). In control experiments, we repeated these experiments with pre-immune serum. UAP56 immunoprecipitates contained the UAP56-interacting protein Aly (**Fig. 6A**), suggesting that the isolated complexes are stable throughout the purification procedure. Indeed, we observed a higher level of *MHC-ftz-Δi* mRNA enrichment in UAP56 immunoprecipitates in comparison to *c-ftz-i* (**Fig. 6B**). To further confirm our results, we compared the enrichment of *MHC-ftz-Δi* mRNA and the 7SL RNA in UAP56 immunoprecipitates. 7SL is a very abundant non-coding RNA that is part of the Signal Recognition Particle (SRP) and is exported to the cytoplasm independently of the TREX-TAP mRNA export pathway.[34] Indeed, while *MHC-ftz-Δi* was enriched in the UAP56 immunoprecipitates, 7SL was not (**Fig. 6C**). From these experiments, we conclude that *MHC-ftz-Δi* associates with UAP56 in vivo.

**The poly(A)-tail is required for the efflux of *MHC-ftz-Δi* mRNA from nuclear speckles.** In yeast, the UAP56 and TAP homologs, Sub2p, and Mex67p, have been shown to affect the retention of hyperpolyadenylated mRNA in nuclear foci.[35] With this in mind, we decided to investigate whether the poly(A)-tail affected how these mRNAs trafficked through speckles. Previously we found that in vitro synthesized *MHC-ftz-Δi* that lacked a poly(A)-tail (*MHC-ftz-Δi-ΔpA)* was rapidly degraded when microinjected into cells.[13] In order to stabilize this RNA, we treated in vitro synthesized *MHC-ftz-Δi-ΔpA* with sodium periodate which selectively oxidizes the vicinal diols on the 2' and 3'carbons of the 3' ribose to form di-aldehydes. This treatment prevents the RNA from being degraded by certain 3'-5'exonucleases.[36] Since the 5'cap is also a substrate for this reaction, we first reacted uncapped RNA with periodate, purified it, and then performed the capping reaction. Indeed, when compared with the non-oxidized mRNA, periodate oxidized *MHC-ftz-Δi-ΔpA* was stable in microinjected U2OS cells (**Fig. 7A**). This mRNA was also poorly exported when compared with microinjected in vitro transcribed and polyadenylated *MHC-ftz-Δi* (**Fig. 7B and C**). This result indicates that the poly(A)-tail is required for ALREX. We then compared the nuclear localization of these mRNAs with SC35. Remarkably, the localization of microinjected oxidized *MHC-ftz-Δi-ΔpA* into nuclear speckles increased dramatically in comparison to in vitro transcribed and polyadenylated *MHC-ftz-Δi* (**Fig. 7D–F**). These results indicate that the poly(A)-tail is required for the efficient efflux of *MHC-ftz-Δi* from nuclear speckles as well as its efficient export to the cytoplasm.

## Discussion

Here we shed further light on the molecular mechanism of the ALREX pathway. Our work indicates that ALREX-promoting elements are sensitive to certain features of the reporter transcript. Two mRNAs that are highly susceptible to ALREX, *ftz,* and *insulin*, are trafficked through nuclear speckles, while a third that is less dependent on ALREX, β*G*, shows weak association with these structures. Our results are consistent with the idea that egress from speckles, and nuclear export, requires two RNA helicases, which are normally associated with the TREX complex (UAP56 and URH49), and the heterodimeric nuclear transport receptor, TAP/p15. Our data suggests that at least some ALREX-promoting elements may be more efficient at recruiting UAP56/URH49 than particular introns, thus explaining why in certain circumstances the ALREX pathway is less sensitive to the depletion of UAP56/URH49 than splicing-dependent export. Finally, our data indicates that the poly(A)-tail is required for efficient nuclear speckle egress, and nuclear export, of *MHC-ftz-Δi* mRNA.

From this data we propose a general model for the trafficking of mRNAs containing ALREX-elements (**Fig. 8**). Our data indicates that mRNAs are first targeted to speckles by several possible routes. Although ALREX-promoting elements and splicing may contribute to this, other features within the transcript likely

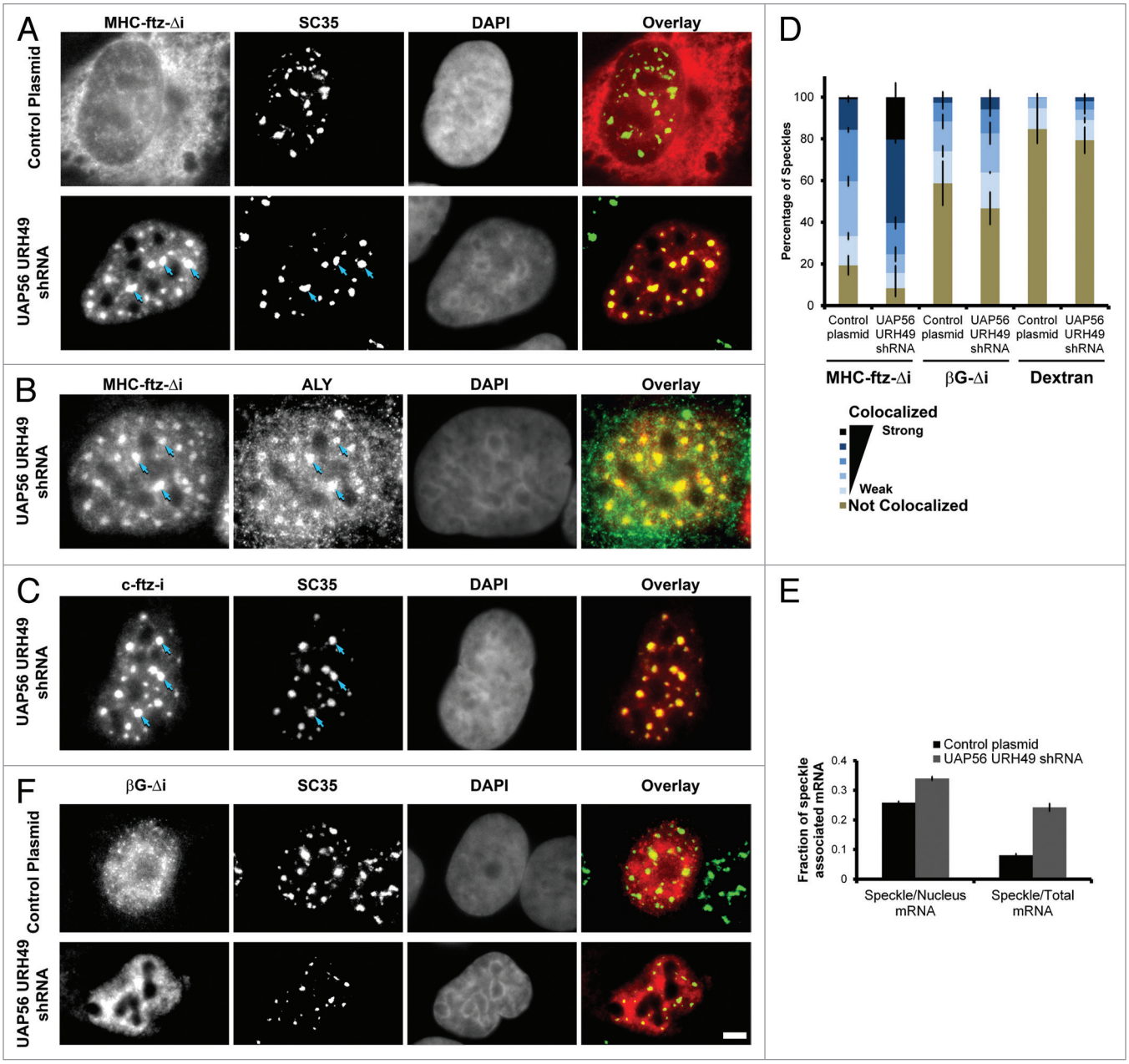


**Figure 4.** Depletion of UAP56 and URH49 causes an enrichment of *MHC-ftz-Δi* mRNA but not *βG-Δi* mRNA in nuclear speckles. (**A–C and F**) U2OS cells were treated with lentiviruses that either mediate the delivery of shRNAs against UAP56 and URH49 or control plasmids. Three days post-infection, cells were microinjected with plasmid containing *MHC-ftz-Δi* (A-B), *c-ftz-i* (**C**) or *βG-Δi* (**F**). After allowing the plasmid to be transcribed for 20 min, cells were treated with α-amanitin and incubated for an additional 2 h. Cells were then fixed, probed for either *ftz* (**A-C**) or *βG* (**F**) mRNA and immunostained for the nuclear speckle markers SC35 (**A, C and F**) or Aly (**B**). Each row represents a single field of view. Overlays of mRNA (red) and SC35 (**A, C and F**) or Aly (**B**) (green) are shown in the right panels. Scale bar = 5 μm. (**D**) The percentage of SC35-positive speckles that colocalize with *MHC-ftz-Δi*, *βG-Δi* mRNA or dextran in control cells or cells depleted of UAP56 and URH49. The data was analyzed and plotted as in **Figure 1D**. (**E**) The percentage of total cellular and nuclear *MHC-ftz-Δi* mRNA that is present in nuclear speckles in control cells or cells depleted of UAP56 and URH49 as described in **Figure 1H**. Each bar represents the average and standard error of the mean of 10 cells.

promote this activity. Within speckles, either ALREX-promoting elements or splicing is sufficient to help assemble the mRNAs into an export-competent mRNP. Our data suggests that this speckle-associated maturation involves several stages. One step is a UAP56/URH49-dependent and involves the recruitment of UAP56, and perhaps URH49, to the transcript. Seeing that these are general export factors, it remains unclear how these proteins are recruited to mRNA containing ALREX-promoting elements and this likely requires additional nuclear factors. It also remains formally possible that speckle-targeting features also promote export, and that ALREX-promoting SSCRs may simply enhance RNA-stability, as we have previously documented.[13] Our data

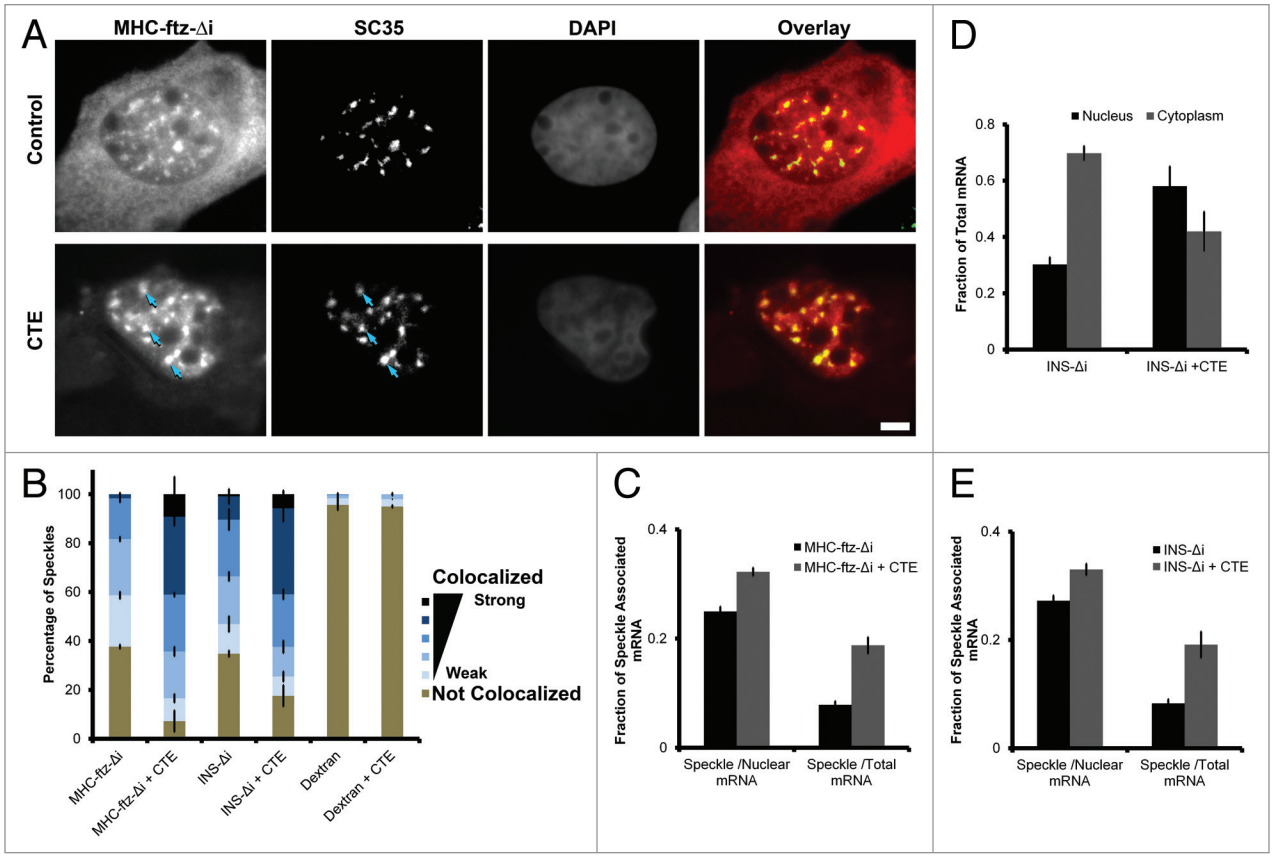


**Figure 5.** TAP inhibition promotes the accumulation of *MHC-ftz-Δi* and *INS-Δi* in nuclear speckles. (**A**) U2OS cells were microinjected with DNA plasmid that codes for *MHC-ftz-Δi* with either in vitro synthesized CTE RNA or control buffer. After allowing the plasmid to be transcribed for 20 min, cells were treated with α-amanitin and incubated for an additional 2 h. Cells were then fixed, probed for *ftz* mRNA and immunostained for the nuclear speckle marker SC35. Each row contains a single field of view with an overlay of the *MHC-ftz-Δi* mRNA (red) and SC35 (green) in the far right panel. Scale bar = 5 μm. (**B**) The percentage of speckles that demonstrate different levels of colocalization with *MHC-ftz-Δi*, *INS-Δi* mRNA or dextran in control cells or cells co-injected with CTE RNA as described in (**A**). The data was analyzed and plotted as in **Figure 1D**. (**C**) The percentage of total cellular and nuclear *MHC-ftz-Δi* mRNA present in nuclear speckles in control cells or cells co-injected with CTE RNA as described in **Figure 1H**. Each bar represents the average and standard error of the mean of 10 cells. (**D**) U2OS cells were either injected with a DNA plasmid that codes for INS-Δi mRNA alone or co-injected in vitro synthesized CTE RNA. After allowing the plasmid to be transcribed for 20 min, cells were treated with α-amanitin and incubated for an additional 2 h. Cells were then fixed, probed for *INS* mRNA and nuclear export was quantified. Each bar represents the average of three independent experiments and error bars represent standard error of the mean. (**E**) The percentage of total cellular and nuclear *INS-Δi* mRNA that is present in nuclear speckles in control cells or cells co-injected with CTE RNA. The data was analyzed and plotted as in **Figure 1H**.

also indicates that there is an additional TAP/p15-dependent step that also occurs within speckles, and likely includes the recruitment of TAP to the mRNA. This step may be coupled with the release of UAP56/URH49,[37,38] although it is possible that UAP56/URH49 may stay on the mRNA and accompany it to the cytoplasm.[39] It is thus likely that egress of export-competent mRNAs from the speckles requires TAP/p15 recruitment, and this is consistent with recent findings.[26] Our data also indicates that one of the speckle-associated steps requires a poly(A)-tail, however its exact role remains unclear.

We have yet to define why certain transcripts, such as *ftz* and *insulin*, have a high degree of speckle-association while others do not. This may be related to certain features that are over-represented in protein coding genes, such as GC-content.[1] It is also clear that many naturally intronless mRNA do not normally associate with speckles,[22,27,28] and this may be due to the requirements of different mRNA export pathways, although it could also be attributable to the fact that these transcripts have a low level of speckle association, but that it is so transient that it is not detectable under normal circumstances. It has also been documented that certain spliced mRNAs do not traffic through speckles yet are still exported to the cytoplasm,[40] although again it is hard to determine whether these mRNAs have a low level of speckle association that is not normally detectable. Although our data supports the model that targeting to nuclear speckles licenses an mRNA for ALREX, thus explaining why *MHC-βG-Δi* mRNA is poorly exported, we do not know whether trafficking through speckles is absolutely required for ALREX.

The role of the poly(A)-tail in nuclear export is unclear at the moment. Many studies have implicated poly(A)-binding proteins in mRNA export,[41-43] while others have found the converse.[44] In budding yeast, components of the TREX-complex have been implicated in the regulation of poly(A)-tail length.[35,45] In particular cases, hyperpolyadenylation, and the subsequent trimming of

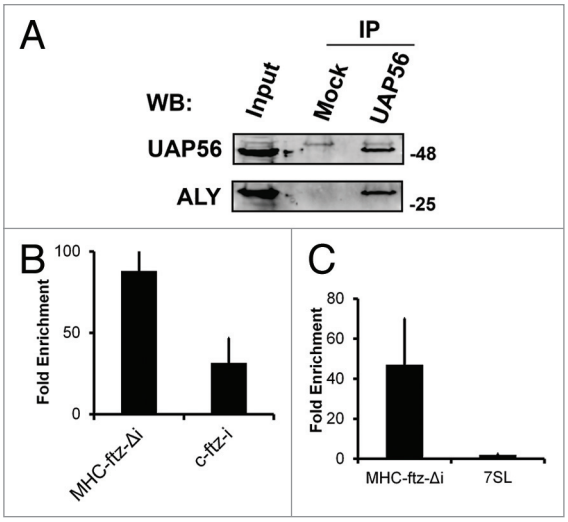


**Figure 6.** *MHC-ftz-Δi* associates with UAP56 in vivo. (**A**) UAP56 was immunoprecipitated from U2OS lysates using rat anti-UAP56 antibodies pre-bound to protein G sepharose. The immunoprecipitates were analyzed by immunoblotting using rabbit polyclonals against UAP56 and Aly. Rat pre-immune serum was used in the mock immunoprecipitation reaction. (**B and C**) U2OS cells were transfected with plasmids containing *MHC-ftz-Δi* (**B and C**) or *c-ftz-i* (**B**). One day after transfection cell lysates were collected and immunoprecipitated with rat anti-UAP56 antibodies or rat pre-immune serum. RNA was collected from fractions and converted to cDNA using *ftz* specific primers (**B**) or random hexamers (**C**). The fold enrichment of mRNAs in anti-UAP56 over pre-immune precipitates was quantified by RT-qPCR. Each bar represents the average of five (**B**) and three (**C**) independent experiments. Error bars represent standard error of the mean.

the poly(A)-tail, is coupled to UAP56 and TAP-dependent steps and may occur in discrete nuclear foci.[35] It however remains unclear whether the poly(A)-tail length is modulated during mRNP assembly in metazoans.

Other work in yeast, indicates that certain mRNPs are rendered export-competent in the vicinity of the nuclear pore.[46-48] This process is initiated by the anchoring of the transcribed gene to the pore in a process known as gene-gating.[49,50] Interestingly, this phenomenon has never been observed in mammalian cells,[51] suggesting that the majority of mRNP formation occurs elsewhere in the nucleoplasm in these organisms. Our data lends support to the notion that in mammalian cells, mRNP formation occurs within speckles. Of course this would require further work identifying critical steps within the mRNP formation pathway, be it directed by splicing or ALREX-promoting elements.

## Materials and Methods

**Plasmid constructs.** The *MHC-ftz-Δi, c-ftz-Δi, c-ftz-i* and *INS-Δi* constructs in pCDNA3 were described previously.[13] Human β*G* introns were amplified from U2OS genomic DNA and inserted into pcDNA3 mammalian expression vector containing β*G* cDNA[52] by restriction-free cloning[53] using the following primer sequences, forward primer: GTGGTGAGGC CCTGGGCAGG TTGGTATCAA GGTTACAAG and the reverse primer: GACCAGCACG TTGCCCAGGA GCTGTGGGAG GAAGATAAG. The mouse *MHC* SSCR, which comprises the first 66 nucleotides from the mouse *H2kb* gene, was first constructed using the following primers—forward primer: CAAAAACTCA TCTCAGAAGA GGATATGGTA CCGTGCACGC TGCTCCTGCT GT and the reverse primer 3: CTCCTCAGGA GTCAGATGCA CCGCGCGGGT CTGAGTCGGA GC. This product was then used in a subsequent PCR reaction to insert the *MHC* SSCR into the β*G*-containing vector by restriction-free cloning. Subsequent to PCR amplification, products were treated with DpnI (New England Biolabs) and incubated at 37 °C for 3–12 h. Products were then purified using PCR purification kits (Qiagen). DH5α *E. coli* cells were transformed with the cloned plasmids. *MHC-ftz-*β*G-Δi*, was constructed by amplifying *MHC-ftz-Δi* using a reverse primer that contained a HindIII site just upstream of the stop codon. This PCR product was digested with HindIII and ligated into β*G-Δi* pCDNA3 that was cut with the same enzyme.

**Cell lines and antibodies.** Both human osteosarcoma (U2OS) and embryonic kidney 293T (HEK293T) were maintained in high glucose DMEM (Wisent) containing 10% FBS (Wisent) and antibiotics (Sigma).

The following antibodies were used: rat polyclonal anti-UAP56,[54] rabbit polyclonal anti-UAP56 (Sigma), rat polyclonal anti-URH49,[54] rabbit polyclonal anti-Aly,[5] rabbit polyclonal anti-THOC1,[3] mouse monoclonal anti-α-tubulin (DM1A, Sigma), mouse monoclonal anti-GAPDH (Millipore), mouse monoclonal anti-HA (Clone HA-7, Sigma) and mouse monoclonal anti-SC35 (Clone SC35, Sigma).

**Lentiviral mediated shRNA protein depletion.** Human embryonic kidney 293 (HEK293T) cells were transiently transfected with gene specific shRNA pLKO.1 plasmids (Sigma) along with the packaging (Δ8.9) and envelope (VSVG) expression vectors[55] using LipoD 293 DNA In Vitro Transfection Reagent (SignaGen Laboratories) following the manufacturer's protocol. Viruses were harvested 48 h after transfection. Human U2OS cells were transduced with viruses in the presence of 8 μg/mL hexadimethrine bromide. One day after transduction, cells were treated with 2 μg/mL Puromycin every other day. The efficiency of the knock-down was assessed 3 d post transduction for UAP56 and URH49 and 4 d for THOC1 and Aly by immunoblotting. The decrease in protein was measured by densitometry analysis, as described previously.[15] These viruses contained the following plasmids obtained from Sigma: TRCN0000074386 (shRNA targeted to UAP56, with sequence CCGGGATAGA CATCTCCTCC TACATCTCGA GATGTAGGAG GAGATGTCTA TCTTTTTG), TRCN0000333247 (shRNA targeted to URH49, with sequence CCGGCCAGGT GATAATCTTC GTCAACTCGA GTTGACGAAG ATTATCACCT GGTTTTTG), TRCN0000272632 (shRNA targeted to THOC1, with sequence CCGGGTGCTC TATTCCAATT GATTACTCGA GTAATCAATT GGAATAGAGC ACTTTTTG), TRCN0000010518 (shRNA targeted to Aly, with sequence CCGGCGTGGA GACAGGTGGG AAACTCTCGA GAGTTTCCCA CCTGTCTCCA CGTTTTT.

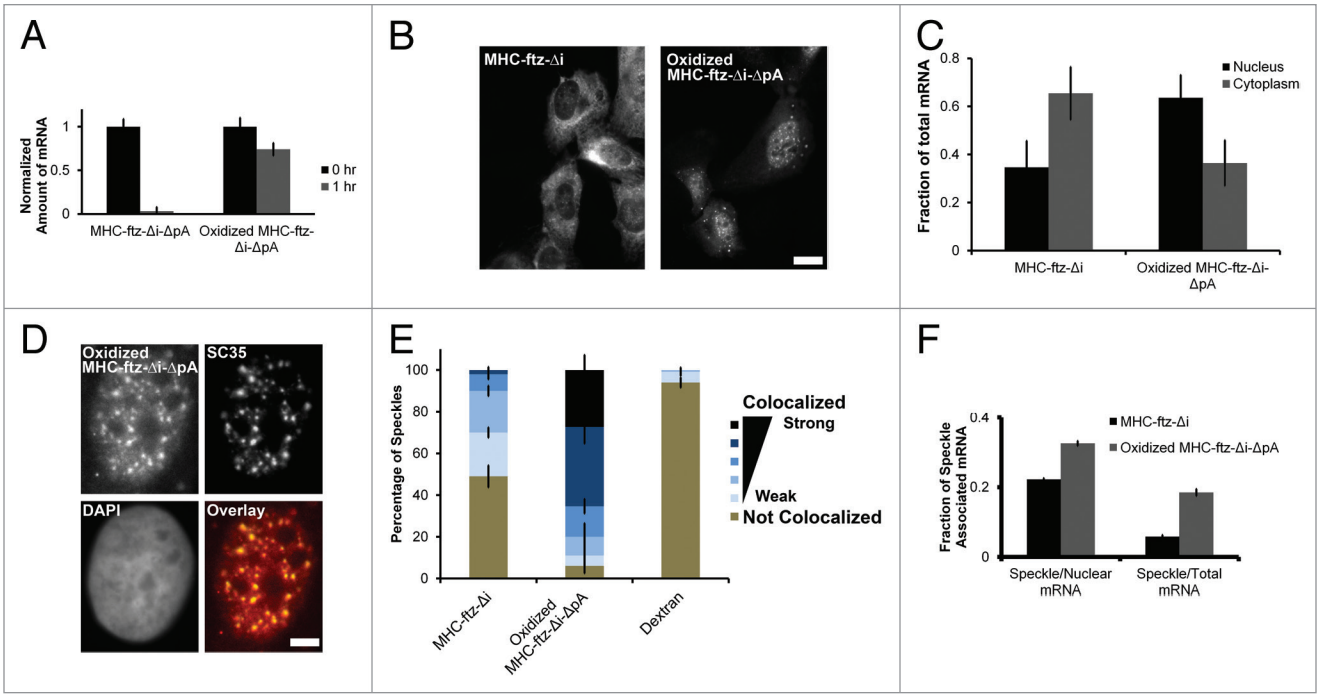


**Figure 7.** *MHC-ftz-Δi* mRNA lacking a poly(A)-tail accumulates in nuclear speckles and is poorly exported. (**A**) In vitro transcribed *MHC-ftz-Δi* mRNA lacking a poly(A)-tail (*ΔpA*) was either oxidized with periodate or left untreated. These mRNAs were microinjected into the nuclei of human U2OS cells, which were then immediately fixed ("0 hr") or first incubated for 1 h at 37°C then fixed. Cells were probed for *ftz* and imaged. The total mRNA fluorescence was quantified for each nuclear-injected cell. Each bar represents the average and standard error of 12–30 cells, all values being normalized to the average fluorescent intensity at 0 h. (**B**) Nuclei of cells were microinjected with either in vitro transcribed and polyadenylated *MHC-ftz-Δi* mRNA or with periodate oxidized *MHC-ftz-Δi-ΔpA*. After allowing mRNA export to proceed for 1 h, cells were fixed, stained using FISH, and imaged. Scale bar = 20 μm. (**C**) The fraction of mRNA in the cytoplasm and nucleus was quantified. Each bar represents the average and standard error of three independent experiments, each consisting of 12–30 cells. (**D**) An example of a nucleus microinjected with in vitro transcribed and oxidized *MHC-ftz-Δi-ΔpA* mRNA and then incubated for 1 h before fixed, probed for *ftz* mRNA and immunostained for the nuclear speckle marker SC35. An overlay of the mRNA (red) and SC35 (green) is shown in the bottom right panel. Scale bar = 5 μm. (**E**) The percentage of nuclear speckles that demonstrate different levels of colocalization with *MHC-ftz-Δi*, periodate oxidized *MHC-ftz-Δi-ΔpA* and dextran 1 h after mRNA microinjection. Data was analyzed and plotted as described in **Figure 1D**. (**F**) The percentage of total cellular and nuclear *MHC-ftz-Δi* and periodate oxidized *MHC-ftz-Δi-ΔpA* mRNA that is present in nuclear speckles as described in **Figure 1H**.

**Microinjection, FISH, and immunostaining.** For microinjection experiments, cells were plated on 22 × 22 mm coverslips (VWR) in 35 mm mammalian tissue culture dishes (Thermo Scientific) for 24 h prior to injection. For DNA microinjections, DNA plasmids were prepared using Qiaprep Midi Kits (Qiagen). Microinjections were performed as previously described.[31] Briefly, DNA plasmids or mRNA transcripts were microinjected at 200 ng/μL with 70 kDa Dextran conjugated to Oregon Green (Invitrogen) and Injection Buffer (100 mM KCl, 10 mM HEPES, pH 7.4). For pulse chase experiments, cells were treated with 1 μg/mL α-amanitin (Sigma) 20 min after injection. After incubating the cells for the appropriate time at 37 °C, they were washed twice with Phosphate Buffer Saline (PBS) and fixed in 4% paraformaldehyde (Electron Microscopy Sciences) in PBS for 15 min. Cells were then permeabilized using 0.1% TritonX-100 in PBS (Thermo Scientific). In HHT experiments, cells were treated with 5 μM HHT (or DMSO as a control) 30 min prior to microinjections. The cells were then maintained in HHT up until they were fixed.

For mRNA staining, cells were washed twice in 1× Sodium Saline Citrate (SSC) buffer supplemented with 60% formamide. Cells were then treated with hybridization buffer (60% formamide, 100 mg/ml dextran sulfate, yeast tRNA, 5 mM VRC, 1× SSC) containing 200nM Alexa 546-conjugated ssDNA probe (Integrated DNA Technologies) for 24 h. Subsequently, coverslips were washed with 1× SSC supplemented with 60% formamide and the coverslips were mounted on DAPI. The probe oligonucleotide sequences included anti-*ftz* (GTCGAGCCTG CCTTTGTCAT CGTCGTCCTT GATAGTCACA ACAGCCGGGA CAACACCCAT), anti-β*G* (CTTCATCCAC GTTCACCTTC GCCCCACAGG GCAGTAACGG CAGACTTCTC CTCAGGAGTC A), or anti-*insulin*, (GGTCCTCTGC CTCCCGGCGG GTCTTGGGTG TGTAGAAGAA GCCTCGTTCC CGCACACACT A). For poly(A) mRNA staining, cells were washed in 1× SSC supplemented with 25% formamide. Cells were treated with poly(A) hybridization buffer (25% formamide, 100 mg/ml dextran sulfate, yeast tRNA, 5 mM VRC, 1× SSC) containing 200 nM Alexa 546-conjugated ssDNA 60mer dT oligonucleotide (Integrated DNA Technologies). For immunostaining, coverslips were first washed with PBS and then blocked with 5% BSA in PBS. Subsequently, proteins were stained with either mouse anti HA antibodies (1:350), mouse anti SC-35 (1:500), rabbit anti

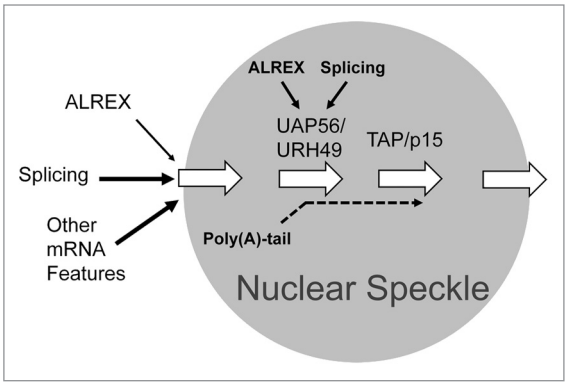


**Figure 8.** Model linking mRNP formation with the trafficking of mRNAs containing ALREX-elements through nuclear speckles. The association of mRNAs with nuclear speckles is promoted by splicing, the presence of an ALREX-promoting element and other unknown features within the mRNA. Within the speckle there are at least two separate steps. The first is dependent on the recruitment of UAP56/URH49 by either splicing and/or ALREX-promoting elements. In addition there is a second downstream step that involves the recruitment of TAP/p15. Finally, the poly(A)-tail is required for the egress of mRNAs containing ALREX-elements from speckles and thus acts at one or several mRNP maturation steps within these structures.

Aly (1:500) or rat anti UAP56 (1:500) for 1 h. Coverslips were washed in PBS and then stained using anti-mouse, anti-rabbit or anti-rat secondary antibodies conjugated to Alexa 647 (1:1500, Molecular Probes) for one hour.

**Imaging and image analysis.** Cells were imaged using a fluorescence microscope (Nikon). Image analysis, including the quantification of mRNA export, was performed using Nikon Imaging Software (NIS) Elements Advanced Research (Nikon) as previously described.[31] For nuclear speckle colocalization analysis, rectangular regions of interest were drawn to cover a single SC35-positive speckle and its surroundings (1–4 $\mu m^2$). Then Pearson correlation ratio between RNA FISH and SC35 immunoflourescence was computed by NIS analysis software. Examples are shown in **Figure 1C**. For each experiment, the 10 brightest SC35-positive speckles per cell were analyzed and the totals from 10 cells were compiled. This analysis was repeated three times and the average and standard error were compiled. The Pearson correlation between microinjected fluorescent dextran and SC35 was also assessed to determine background levels of correlation.

To calculate the fraction of mRNA in speckles, thresholds were drawn on the SC35 immunofluorescence channel using NIS. The threshold was set so that 20% (± 0.5%) of the nuclear area was selected per cell and the fluorescence intensity of RNA in the selected area was calculated. The total integrated mRNA signals in the nucleus and the cell body were also computed.

**In vitro *MHC-ftz-Δi* mRNA synthesis, polyadenylation, capping and periodate oxidization.** pcDNA3 plasmid containing *MHC-ftz-Δi* was linearized by XhoI digestion and precipitated at -80°C for 1 h with 40 mM Potassium Acetate and 2.5× 100% ethanol. The precipitated DNA was resuspended in RNase free water and used as a template to synthesize mRNA using T7 RNA polymerase (NEB) by incubation with 10 mM ATP, 10 mM GTP, 10mM CTP, 10mM UTP for 4 h at 37 °C. Polyadenylation was performed using *E. coli* Poly A Polymerase (NEB) following the manufacturer's protocol. To oxidize the 3'end, 500 pmoles of T7-transcribed RNA previously dissolved in 40 μl of water was added to 360 μl of freshly prepared 5mM Sodium-Periodate (Sigma). The 400 μl reaction mixture was rotated for 1 h in the dark at room temperature. The oxidized RNA was purified by Purelink RNA purification kit (Ambion) and eluted in 30 μl of RNase free water. Oxidized and non-oxidized RNA was capped using vaccinia capping enzyme (NEB) following the manufacturer's protocol and purified by Purelink RNA purification kit (Ambion). RNA was then precipitated at –80°C for 1 h with 40 mM Potassium Acetate and 2.5× 100% ethanol and resuspended in injection buffer.

**CTE mRNA synthesis.** CTE-PCR3.1 plasmid[13] was linearized by Xhol digestion and precipitated at -80°C for 1 h with 40 mM KAcetate and 2.5× 100% ethanol. The precipitated DNA was resuspended in RNase free water. mRNA synthesis and capping was performed by T7 RNA polymerase (NEB) and Vaccinia capping enzyme (NEB). RNA was purified by Purelink RNA purification kit (Ambion), then precipitated at –80°C for 1 h with 40 mM Potassium Acetate and 2.5× 100% ethanol and resuspended in injection buffer.

**RNA immunoprecipitation.** Human U2OS cells were transfected with different *ftz* plasmids using GenJet in vitro DNA Transfection Reagent for U2OS (SignaGen Laboratories). After 18–24 h, cell lysate was incubated for 10–14 h with rat anti-UAP56 antibodies[54] prebound to protein G sepharose (Invitrogen). Subsequently, the beads were washed five times. The RNA is eluted from the UAP56 bound beads using SDS and harvested using Trizol (Invitrogen) as previously described.[56,57] The RNA samples were treated with DNase (Ambion) to remove DNA plasmid contamination. cDNA was synthesized using SuperScript III (Invitrogen) according to the manufacturer's protocol. qPCR was performed by mixing the cDNA with Power Sybr Green Master Mix (Invitrogen) and the reaction was run on a CFX384 Touch Real Time PCR Detection System (Bio-Rad). The efficiency of the IP reaction was checked by immunoblotting with rabbit anti-UAP56 antibodies (Sigma) and rabbit anti-Aly antibodies.[5]

### Disclosure of Potential Conflicts of Interest

No potential conflict of interest was disclosed.

### Supplemental Materials

Supplemental materials may be found here:
www.landesbioscience.com/journals/nucleus/article/26052

### Acknowledgments

We would like to thank H Lipshitz for allowing us to use equipment, A Wilde for providing us with reagents and C Enenkel for providing us with feedback. We would also like to thank C Smibert for providing technical help, various reagents and comments on the manuscript. This work was supported by a grant from the Canadian Institutes of Health Research to AFP (FRN 102725) and an Ontario Graduate Scholarship to AA.

## References


1. Palazzo AF, Akef A. Nuclear export as a key arbiter of "mRNA identity" in eukaryotes. Biochim Biophys Acta 2012; 1819:566-77; PMID:22248619; http://dx.doi.org/10.1016/j.bbagrm.2011.12.012
2. Luo MJ, Reed R. Splicing is required for rapid and efficient mRNA export in metazoans. Proc Natl Acad Sci U S A 1999; 96:14937-42; PMID:10611316; http://dx.doi.org/10.1073/pnas.96.26.14937
3. Masuda S, Das R, Cheng H, Hurt E, Dorman N, Reed R. Recruitment of the human TREX complex to mRNA during splicing. Genes Dev 2005; 19:1512-7; PMID:15998806; http://dx.doi.org/10.1101/gad.1302205
4. Cheng H, Dufu K, Lee C-S, Hsu JL, Dias A, Reed R. Human mRNA export machinery recruited to the 5' end of mRNA. Cell 2006; 127:1389-400; PMID:17190602; http://dx.doi.org/10.1016/j.cell.2006.10.044
5. Zhou Z, Luo MJ, Straesser K, Katahira J, Hurt E, Reed R. The protein Aly links pre-messenger-RNA splicing to nuclear export in metazoans. Nature 2000; 407:401-5; PMID:11014198; http://dx.doi.org/10.1038/35030160
6. Luo ML, Zhou Z, Magni K, Christoforides C, Rappsilber J, Mann M, Reed R. Pre-mRNA splicing and mRNA export linked by direct interactions between UAP56 and Aly. Nature 2001; 413:644-7; PMID:11675789; http://dx.doi.org/10.1038/35098106
7. Strässer K, Masuda S, Mason P, Pfannstiel J, Oppizzi M, Rodriguez-Navarro S, Rondón AG, Aguilera A, Struhl K, Reed R, et al. TREX is a conserved complex coupling transcription with messenger RNA export. Nature 2002; 417:304-8; PMID:11979277; http://dx.doi.org/10.1038/nature746
8. Chang C-T, Hautbergue GM, Walsh MJ, Viphakone N, van Dijk TB, Philipsen S, Wilson SA. Chtop is a component of the dynamic TREX mRNA export complex. EMBO J 2013; 32:473-86; PMID:23299939; http://dx.doi.org/10.1038/emboj.2012.342
9. Viphakone N, Hautbergue GM, Walsh M, Chang CT, Holland A, Folco EG, Reed R, Wilson SA. TREX exposes the RNA-binding domain of Nxf1 to enable mRNA export. Nat Commun 2012; 3:1006; PMID:22893130; http://dx.doi.org/10.1038/ncomms2005
10. Segref A, Sharma K, Doye V, Hellwig A, Huber J, Lührmann R, Hurt E. Mex67p, a novel factor for nuclear mRNA export, binds to both poly(A)+ RNA and nuclear pores. EMBO J 1997; 16:3256-71; PMID:9214641; http://dx.doi.org/10.1093/emboj/16.11.3256
11. Katahira J, Strässer K, Podtelejnikov A, Mann M, Jung JU, Hurt E. The Mex67p-mediated nuclear mRNA export pathway is conserved from yeast to human. EMBO J 1999; 18:2593-609; PMID:10228171; http://dx.doi.org/10.1093/emboj/18.9.2593
12. Strässer K, Hurt E. Yra1p, a conserved nuclear RNA-binding protein, interacts directly with Mex67p and is required for mRNA export. EMBO J 2000; 19:410-20; PMID:10722314; http://dx.doi.org/10.1093/emboj/19.3.410
13. Palazzo AF, Springer M, Shibata Y, Lee C-S, Dias AP, Rapoport TA. The signal sequence coding region promotes nuclear export of mRNA. PLoS Biol 2007; 5:e322; PMID:18052610; http://dx.doi.org/10.1371/journal.pbio.0050322
14. Cenik C, Chua HN, Zhang H, Tarnawsky SP, Akef A, Derti A, Tasan M, Moore MJ, Palazzo AF, Roth FP. Genome analysis reveals interplay between 5'UTR introns and nuclear mRNA export for secretory and mitochondrial genes. PLoS Genet 2011; 7:e1001366; PMID:21533221; http://dx.doi.org/10.1371/journal.pgen.1001366
15. Mahadevan K, Zhang H, Akef A, Cui XA, Gueroussov S, Cenik C, Roth FP, Palazzo AF. RanBP2/Nup358 potentiates the translation of a subset of mRNAs encoding secretory proteins. PLoS Biol 2013; 11:e1001545; PMID:23630457
16. Spector DL, Lamond AI. Nuclear speckles. Cold Spring Harb Perspect Biol 2011; 3:a000646; PMID:20926517; http://dx.doi.org/10.1101/cshperspect.a000646
17. Kota KP, Wagner SR, Huerta E, Underwood JM, Nickerson JA. Binding of ATP to UAP56 is necessary for mRNA export. J Cell Sci 2008; 121:1526-37; PMID:18411249; http://dx.doi.org/10.1242/jcs.021055
18. Dufu K, Livingstone MJ, Seebacher J, Gygi SP, Wilson SA, Reed R. ATP is required for interactions between UAP56 and two conserved mRNA export proteins, Aly and CIP29, to assemble the TREX complex. Genes Dev 2010; 24:2043-53; PMID:20844015; http://dx.doi.org/10.1101/gad.1898610
19. Wang J, Cao LG, Wang YL, Pederson T. Localization of pre-messenger RNA at discrete nuclear sites. Proc Natl Acad Sci U S A 1991; 88:7391-5; PMID:1831271; http://dx.doi.org/10.1073/pnas.88.16.7391
20. Melcák I, Melcáková S, Kopský V, Vecerová J, Raska I. Prespliceosomal assembly on microinjected precursor mRNA takes place in nuclear speckles. Mol Biol Cell 2001; 12:393-406; PMID:11179423; http://dx.doi.org/10.1091/mbc.12.2.393
21. Tokunaga K, Shibuya T, Ishihama Y, Tadakuma H, Ide M, Yoshida M, Funatsu T, Ohshima Y, Tani T. Nucleocytoplasmic transport of fluorescent mRNA in living mammalian cells: nuclear mRNA export is coupled to ongoing gene transcription. Genes Cells 2006; 11:305-17; PMID:16483318; http://dx.doi.org/10.1111/j.1365-2443.2006.00936.x
22. Dias AP, Dufu K, Lei H, Reed R. A role for TREX components in the release of spliced mRNA from nuclear speckle domains. Nat Commun 2010; 1:97; PMID:20981025; http://dx.doi.org/10.1038/ncomms1103
23. Vargas DY, Shah K, Batish M, Levandoski M, Sinha S, Marras SA, Schedl P, Tyagi S. Single-molecule imaging of transcriptionally coupled and uncoupled splicing. Cell 2011; 147:1054-65; PMID:22118462; http://dx.doi.org/10.1016/j.cell.2011.10.024
24. Schmidt U, Richter K, Berger AB, Lichter P. In vivo BiFC analysis of Y14 and NXF1 mRNA export complexes: preferential localization within and around SC35 domains. J Cell Biol 2006; 172:373-81; PMID:16431928; http://dx.doi.org/10.1083/jcb.200503061
25. Daguenet E, Baguet A, Degot S, Schmidt U, Alpy F, Wendling C, Spiegelhalter C, Kessler P, Rio MC, Le Hir H, et al. Perispeckles are major assembly sites for the exon junction core complex. Mol Biol Cell 2012; 23:1765-82; PMID:22419818; http://dx.doi.org/10.1091/mbc.E12-01-0040
26. Teng I-F, Wilson SA. Mapping Interactions between mRNA Export Factors in Living Cells. PLoS One 2013; 8:e67676; PMID:23826332; http://dx.doi.org/10.1371/journal.pone.0067676
27. Lei H, Dias AP, Reed R. Export and stability of naturally intronless mRNAs require specific coding region sequences and the TREX mRNA export complex. Proc Natl Acad Sci U S A 2011; 108:17985-90; PMID:22010220; http://dx.doi.org/10.1073/pnas.1113076108
28. Lei H, Zhai B, Yin S, Gygi S, Reed R. Evidence that a consensus element found in naturally intronless mRNAs promotes mRNA export. Nucleic Acids Res 2013; 41:2517-25; PMID:23275560; http://dx.doi.org/10.1093/nar/gks1314
29. Fu XD, Maniatis T. Factor required for mammalian spliceosome assembly is localized to discrete regions in the nucleus. Nature 1990; 343:437-41; PMID:2137203; http://dx.doi.org/10.1038/343437a0
30. Spector DL, Fu XD, Maniatis T. Associations between distinct pre-mRNA splicing components and the cell nucleus. EMBO J 1991; 10:3467-81; PMID:1833187
31. Gueroussov S, Tarnawsky SP, Cui XA, Mahadevan K, Palazzo AF. Analysis of mRNA nuclear export kinetics in mammalian cells by microinjection. J Vis Exp 2010; 46:2387; PMID:21178962
32. Kapadia F, Pryor A, Chang T-H, Johnson LF. Nuclear localization of poly(A)+ mRNA following siRNA reduction of expression of the mammalian RNA helicases UAP56 and URH49. Gene 2006; 384:37-44; PMID:16949217; http://dx.doi.org/10.1016/j.gene.2006.07.010
33. Bachi A, Braun IC, Rodrigues JP, Panté N, Ribbeck K, von Kobbe C, Kutay U, Wilm M, Görlich D, Carmo-Fonseca M, et al. The C-terminal domain of TAP interacts with the nuclear pore complex and promotes export of specific CTE-bearing RNA substrates. RNA 2000; 6:136-58; PMID:10668806; http://dx.doi.org/10.1017/S1355838200991994
34. Grosshans H, Deinert K, Hurt E, Simos G. Biogenesis of the signal recognition particle (SRP) involves import of SRP proteins into the nucleolus, assembly with the SRP-RNA, and Xpo1p-mediated export. J Cell Biol 2001; 153:745-62; PMID:11352936; http://dx.doi.org/10.1083/jcb.153.4.745
35. Kallehauge TB, Robert M-C, Bertrand E, Jensen TH. Nuclear retention prevents premature cytoplasmic appearance of mRNA. Mol Cell 2012; 48:145-52; PMID:22921936; http://dx.doi.org/10.1016/j.molcel.2012.07.022
36. Aphasizhev R, Simpson L. Isolation and characterization of a U-specific 3'-5'-exonuclease from mitochondria of Leishmania tarentolae. J Biol Chem 2001; 276:21280-4; PMID:11279235; http://dx.doi.org/10.1074/jbc.M100297200
37. Taniguchi I, Ohno M. ATP-dependent recruitment of export factor Aly/REF onto intronless mRNAs by RNA helicase UAP56. Mol Cell Biol 2008; 28:601-8; PMID:17984224; http://dx.doi.org/10.1128/MCB.01341-07
38. Hautbergue GM, Hung M-L, Golovanov AP, Lian L-Y, Wilson SA. Mutually exclusive interactions drive handover of mRNA from export adaptors to TAP. Proc Natl Acad Sci U S A 2008; 105:5154-9; PMID:18364396; http://dx.doi.org/10.1073/pnas.0709167105
39. Thomas M, Lischka P, Müller R, Stamminger T. The cellular DExD/H-box RNA-helicases UAP56 and URH49 exhibit a CRM1-independent nucleocytoplasmic shuttling activity. PLoS One 2011; 6:e22671; PMID:21799930; http://dx.doi.org/10.1371/journal.pone.0022671
40. Smith KP, Moen PT, Wydner KL, Coleman JR, Lawrence JB. Processing of endogenous pre-mRNAs in association with SC-35 domains is gene specific. J Cell Biol 1999; 144:617-29; PMID:10037785; http://dx.doi.org/10.1083/jcb.144.4.617
41. Hector RE, Nykamp KR, Dheur S, Anderson JT, Non PJ, Urbinati CR, Wilson SM, Minvielle-Sebastia L, Swanson MS. Dual requirement for yeast hnRNP Nab2p in mRNA poly(A) tail length control and nuclear export. EMBO J 2002; 21:1800-10; PMID:11927564; http://dx.doi.org/10.1093/emboj/21.7.1800
42. Farny NG, Hurt JA, Silver PA. Definition of global and transcript-specific mRNA export pathways in metazoans. Genes Dev 2008; 22:66-78; PMID:18086857; http://dx.doi.org/10.1101/gad.1616008
43. Hurt JA, Obar RA, Zhai B, Farny NG, Gygi SP, Silver PA. A conserved CCCH-type zinc finger protein regulates mRNA nuclear adenylation and export. J Cell Biol 2009; 185:265-77; PMID:19364924; http://dx.doi.org/10.1083/jcb.200811072
44. Bhattacharjee RB, Bag J. Depletion of nuclear poly(A) binding protein PABPN1 produces a compensatory response by cytoplasmic PABP4 and PABP5 in cultured human cells. PLoS One 2012; 7:e53036; PMID:23300856; http://dx.doi.org/10.1371/journal.pone.0053036

45. Vinciguerra P, Iglesias N, Camblong J, Zenklusen D, Stutz F. Perinuclear Mlp proteins downregulate gene expression in response to a defect in mRNA export. EMBO J 2005; 24:813-23; PMID:15692572; http://dx.doi.org/10.1038/sj.emboj.7600527
46. Cabal GG, Genovesio A, Rodriguez-Navarro S, Zimmer C, Gadal O, Lesne A, Buc H, Feuerbach-Fournier F, Olivo-Marin JC, Hurt EC, et al. SAGA interacting factors confine sub-diffusion of transcribed genes to the nuclear envelope. Nature 2006; 441:770-3; PMID:16760982; http://dx.doi.org/10.1038/nature04752
47. Fasken MB, Stewart M, Corbett AH. Functional significance of the interaction between the mRNA-binding protein, Nab2, and the nuclear pore-associated protein, Mlp1, in mRNA export. J Biol Chem 2008; 283:27130-43; PMID:18682389; http://dx.doi.org/10.1074/jbc.M803649200
48. Pascual-García P, Govind CK, Queralt E, Cuenca-Bono B, Llopis A, Chavez S, Hinnebusch AG, Rodríguez-Navarro S. Sus1 is recruited to coding regions and functions during transcription elongation in association with SAGA and TREX2. Genes Dev 2008; 22:2811-22; PMID:18923079; http://dx.doi.org/10.1101/gad.483308
49. Casolari JM, Brown CR, Komili S, West J, Hieronymus H, Silver PA. Genome-wide localization of the nuclear transport machinery couples transcriptional status and nuclear organization. Cell 2004; 117:427-39; PMID:15137937; http://dx.doi.org/10.1016/S0092-8674(04)00448-9
50. Brickner JH. Transcriptional memory at the nuclear periphery. Curr Opin Cell Biol 2009; 21:127-33; PMID:19181512; http://dx.doi.org/10.1016/j.ceb.2009.01.007
51. Hocine S, Singer RH, Grünwald D. RNA processing and export. Cold Spring Harb Perspect Biol 2010; 2:a000752; PMID:20961978; http://dx.doi.org/10.1101/cshperspect.a000752
52. Valencia P, Dias AP, Reed R. Splicing promotes rapid and efficient mRNA export in mammalian cells. Proc Natl Acad Sci U S A 2008; 105:3386-91; PMID:18287003; http://dx.doi.org/10.1073/pnas.0800250105
53. van den Ent F, Löwe J. RF cloning: a restriction-free method for inserting target genes into plasmids. J Biochem Biophys Methods 2006; 67:67-74; PMID:16480772; http://dx.doi.org/10.1016/j.jbbm.2005.12.008
54. Yamazaki T, Fujiwara N, Yukinaga H, Ebisuya M, Shiki T, Kurihara T, Kioka N, Kambe T, Nagao M, Nishida E, et al. The closely related RNA helicases, UAP56 and URH49, preferentially form distinct mRNA export machineries and coordinately regulate mitotic progression. Mol Biol Cell 2010; 21:2953-65; PMID:20573985; http://dx.doi.org/10.1091/mbc.E09-10-0913
55. Ma XM, Yoon S-O, Richardson CJ, Jülich K, Blenis J. SKAR links pre-mRNA splicing to mTOR/S6K1-mediated enhanced translation efficiency of spliced mRNAs. Cell 2008; 133:303-13; PMID:18423201; http://dx.doi.org/10.1016/j.cell.2008.02.031
56. Keene JD, Komisarow JM, Friedersdorf MB. RIP-Chip: the isolation and identification of mRNAs, microRNAs and protein components of ribonucleoprotein complexes from cell extracts. Nat Protoc 2006; 1:302-7; PMID:17406249; http://dx.doi.org/10.1038/nprot.2006.47
57. Laver JD, Ancevicius K, Sollazzo P, Westwood JT, Sidhu SS, Lipshitz HD, Smibert CA. Synthetic antibodies as tools to probe RNA-binding protein function. Mol Biosyst 2012; 8:1650-7; PMID:22481296; http://dx.doi.org/10.1039/c2mb00007e